

Hydration and saccharification of cellulose I β , II and III $_1$ at increasing dry solids loadings

Michael J. Selig · Lisbeth G. Thygesen ·
David K. Johnson · Michael E. Himmel ·
Claus Felby · Ashutosh Mittal

Received: 8 March 2013 / Accepted: 24 May 2013 / Published online: 24 July 2013
© Springer Science+Business Media Dordrecht 2013

Abstract Crystalline cellulose I β (Avicel) was chemically transformed into cellulose II and III $_1$ producing allomorphs with similar crystallinity indices (ATR-IR and XRD derived). Saccharifications by commercial cellulases at arrayed solids loadings showed cellulose III $_1$ was more readily hydrolysable and less susceptible to increased dry solids levels than cellulose I β and II. Analysis by dynamic vapor sorption revealed cellulose II has a distinctively higher absorptive capacity than cellulose I and III $_1$. When equally hydrated (g water/g cellulose), low-field nuclear magnetic resonance (LF-NMR) relaxometry showed that cellulose II, on average, most constrained water while cellulase III $_1$ left the most free water. LF-NMR spin–spin relaxation time distribution profiles representing distinct water pools suggest cellulose III $_1$ had the most restricted pool and changes in water distribution during enzymatic saccharification were most dramatic with respect to cellulose III $_1$ compared to celluloses I β and II.

Keywords Cellulose · Crystalline allomorph · High solids · Hydration · Saccharification

Introduction

In the biomass conversion industry, the primary target of fermentation processes aims at utilizing the structural carbohydrates in lignocellulosic feedstocks remains the glucose monomers in crystalline cellulose. While abundant in nature, the tightly hydrogen-bonded structure and the partially hydrophobic nature of the polymer makes enzymatic conversions difficult and slow requiring the effective synergy of multiple cellulase enzymes to extensively utilize the substrate. In addition to the obstacles presented by the crystalline nature of the cellulose polymer itself, the intermeshed network of pectins, cross-linking glycans, lignins and silicates in lignocelluloses poses numerous limitations to enzymatic access and deconstruction rates (and extents). Overcoming these limitations has often been the basis for inclusion of hydrothermal and thermochemical pretreatment steps in most proposed second generation biomass conversion schemes.

Cellulose in plant cell walls predominately exists in a form called I β . It is composed of alternating sheets of β -1,4-linked glycan chains offset by half a glucose molecule. During plant cell wall biosynthesis individual glycans and sheets of glycans are driven together

M. J. Selig (✉) · L. G. Thygesen · C. Felby
Department of Forest & Landscape, Faculty of Science,
University of Copenhagen, Rolighedsvej 23,
1958 Frederiksberg, Denmark
e-mail: mjs@life.ku.dk

D. K. Johnson · M. E. Himmel · A. Mittal
National Renewable Energy Laboratory, 1617 Cole Blvd,
Golden, CO 80401, USA
e-mail: Ashutosh.Mittal@nrel.gov

by hydrophobic interactions and van der Waals forces and bound tightly by stable glycan–glycan hydrogen bonds to form a strong crystalline structure (Matthews et al. 2006). Disruption followed by an alteration of the hydrogen-bonding pattern amongst the glycan chains is thought to occur during some chemical treatments of lignocelluloses; particularly those utilizing base and ammonia (Mittal et al. 2011). This reorganization into alternate crystalline forms is thought to help reduce the resistance to enzymatic degradation by changing the free energies of decrystallization, altering effective binding of critical enzymes, and the related organization of water saturating the crystalline surfaces (Igarashi et al. 2007; Chundawat et al. 2011).

Likewise, the hydration of cellulose (and lignocelluloses) is thought to critically impact the effectiveness of enzymatic hydrolysis. This is particularly the case in industrial processes where high dry solids loadings of up to 40 % (w/w) can be necessary to achieve economic viability. At high dry solids loadings a greater fraction of the water present is associated with biomass surfaces and, in general, this association increases the overall constraint and availability of the water in a system. These factors are affected by increased concentrations of both insoluble and water soluble components and need to be considered during lignocellulose conversion process design (Roberts et al. 2011; Selig et al. 2012). Previous studies using cellulose I β as a model substrate have attempted to characterize the distribution of water at increased solids loadings during traditional enzymatic hydrolysis by delineating between three major groupings of water with respect to how constrained their movement is in a system; water bound to the cellulose surface (bound—most constrained for insoluble solids; less constrained when bound to soluble compounds), unbound water that is restricted to capillary spaces (capillary restricted—significantly constrained), and free water (Felby et al. 2008; Roberts et al. 2011). In a similar respect, little attention has been given to how water is organized in systems of alternate cellulose allomorphs and here we aim to explore this in hopes of better understanding the differences in conversion rates that are known to exist.

This body of work investigates the comparative hydration of cellulose with respect to varied crystalline forms; specifically those identified as I β , II, and III $_1$. The three allomorphs were prepared chemically from the same stock of Avicel pH 101 (I β cellulose;

Sigma-Aldrich) to similar degrees of crystallinity. Observations on the hydration of the three allomorphs were then made via dynamic vapour sorption (DVS) and low-field nuclear magnetic resonance (LF-NMR) methods. We specifically observed cellulose/water systems in the LF-NMR at 10 and 30 % (w/w) dry solids levels and further observe saccharification of the allomorphs in the same system at 10 % (w/w) dry solids. These hydration data are then compared to enzymatic saccharifications of the celluloses at increasing dry solids loadings. Overall, the study provides insight into the potential importance of hydration during cellulose saccharification, particularly at increased dry matter loadings where water availability becomes limited.

Materials and methods

Preparation of cellulose samples

All celluloses were prepared from cellulose I β (Avicel PH 101, catalog number 11,365) at the National Renewable Energy Laboratory (NREL) in Golden, Colorado, USA. Amorphous cellulose was prepared in a planetary ball mill (Retsh model PM100, Haan, Germany) for 6 h at 25 °C and at 600 rpm using ZrO $_2$ bowls (volume = 50 ml) and nine ZrO $_2$ balls employing a 5 min on and 5 min off cycle, amorphous state was verified by X-ray diffraction (XRD).

Cellulose II was prepared by aqueous NaOH treatment as described by Atalla (1974). Briefly, Avicel was stirred in 23 % (w/w) NaOH at 5 g Avicel per 100 g NaOH solution at 25 °C for 50 min under N $_2$. The solution was diluted to 17.5 % (w/w) NaOH, heated at 70 °C for 50 min, and then similarly heated at 70 °C for successive NaOH concentrations of 15, 12, 10, 8, 4, and 1 % (w/w). The cellulose was extensively washed with deionized water at 70 °C to obtain a pH of ~7, filtered to dewater, and then immersed in glycerol at 100 °C in a stainless steel reaction vessel (Parr Instrument Co., Model 4520, Moline, IL) and heated at 145 °C for 7 days; following the cellulose was washed with boiling deionized water and freeze dried; this was designated as cellulose II (145 °C).

Cellulose III $_1$ was prepared according to Mittal et al. (2011). Briefly, cellulose I was placed in a stainless-steel reaction vessel (Parr Instrument Company, Model 4714, Moline, IL) and chilled in a dry ice

and acetone bath at $-75\text{ }^{\circ}\text{C}$. Anhydrous liquid ammonia was added slowly at a ratio of 2.5 g ammonia per cellulose, cooled at $-75\text{ }^{\circ}\text{C}$ for 15 min, and then held at $25\text{ }^{\circ}\text{C}$ for 30 min. The vessel was then placed in a preheated fluidized sand bath maintained at $130\text{ }^{\circ}\text{C}$ for 1 h. After 1 h the vessel was depressurized by allowing the ammonia to leak out in a ventilated hood and cooled in a $25\text{ }^{\circ}\text{C}$ water-bath. The resulting cellulose III_I was removed from the vessel and left in the hood overnight until all the ammonia had evaporated.

X-ray diffraction measurements

The crystallinity indexes (CI) of cellulose samples were measured by XRD by using a Rigaku (Tokyo, Japan) Ultima IV diffractometer with $\text{CuK}\alpha$ radiation having a wavelength $\lambda(\text{K}\alpha 1) = 0.15406\text{ nm}$ generated at 40 kV and 44 mA. The diffraction intensities of freeze dried samples placed on a quartz substrate were measured in the range of $8\text{--}42^{\circ} 2\theta$ using a step size of 0.02° at a rate of $2^{\circ}/\text{min}$. The CI were calculated according to the amorphous subtraction method described by Park et al. (2009, 2011). Briefly, a diffractogram of a sample of the prepared amorphous cellulose was subtracted from the diffractograms of the other cellulose samples and then the ratio of the integrated area of each subtracted diffractogram to the area of the original diffractogram was calculated and multiplied by 100.

ATR-IR analysis of celluloses

Cellulose allomorphs were analyzed on a Thermo Nicolet 6700 FT-IR spectrometer equipped with a temperature adjustable ATR (Golden Gate) component (purged with dry air) to reconfirm that crystallinity levels of the three celluloses were similar. Spectra were taken at 4 cm^{-1} resolution after 128 scans; the background baseline was collected after 256 scans. The distortion associated with dispersion effects on IR band positions was corrected for by applying the advanced ATR correction in the spectrometer Omnic software. Spectra for five replicate samples were taken for each cellulose allomorph. The standard normal variate transformation described by Barnes et al. (1989) was applied to all replicate spectra; an average of all replicates is presented. Total crystallinity indices (TCI) calculated by taking the ratio of peak intensities at $1,372$ and $2,900\text{ cm}^{-1}$ and

the lateral order index (LOI) by the ratio of peak intensities at $1,429$ and 893 cm^{-1} .

Enzymatic saccharifications

All enzymatic saccharifications were performed at $48\text{ }^{\circ}\text{C}$ in 50 mM sodium citrate buffer, pH 4.8, in 2.0 ml Eppendorf tubes. Initial solids loadings of 1, 5 and 10 % (w/w) were run for 24 h. Novozymes' (Bagsværd, Denmark) Cellic Ctec2 commercial cellulase was used at 10 mg/g cellulose for all digestions. Upon sampling, the 1 and 5 % solids saccharifications were diluted 1 in 2 parts and the 10 % solids digestions were diluted 1 in 4 parts. Glucose in the diluted hydrolysates was determined by HPLC with a Rezex ROA Organic Acids H+ column (Phenomenex; Torrance, CA) using 0.5 % sulfuric acid at 0.6 ml/min as eluent.

Dynamic vapor sorption of celluloses

Dynamic vapor sorption tests were run on $\sim 1.5\text{ mg}$ of each cellulose in a QA 5000 SA vapor sorption system from Prager Elektronik (Wolkersdorf, Germany). Samples were stored in open containers in a desiccator overnight prior to analysis. Once in the humidity chamber the samples were first equilibrated at 0 % humidity for 3 h. Afterwards humidity was introduced to the control and sample chambers at a constant rate of 0.1 % per min until the maximum of 97 % was achieved. After this time the full humidity levels were maintained for an additional 1.5 h. This procedure implies that the absorption isotherms recorded do not reflect equilibrium conditions but rather express qualitative differences in the sorption behavior of the three different cellulose allomorphs, i.e. the rate at which they accommodate moisture into their structure when exposed to slowly increasing humidity levels.

Cellulose hydration analyzed by low-field NMR

LF-NMR was performed on a Bruker mq20 minispec with a 0.47 Tesla permanent magnet equivalent to a 20 MHz proton resonance frequency. The magnet temperature was held at $40\text{ }^{\circ}\text{C}$ for all measurements and spin–spin transverse, T_2 , relaxation times were determined using the Carr–Purcell–Meiboom–Gill (CPMG) sequence. For all runs 32 scans were acquired using a 5 s recycle delay; 8,000 echoes were collected with a pulse separation of 0.05 ms for each

scan. The CONTIN Laplace transformation method described by Provencher (1982) was utilized to determine relaxation time distributions from the CPMG curves. All NMR data and observations were verified by repeated experimental sets.

Results and discussion

Analysis of celluloses

Similar levels of crystallinity between the cellulose allomorphs were confirmed by both XRD and ATR-IR

spectra (Fig. 1) and the related crystallinity indices are reported in Table 1. The IR derived LOI is specifically indicative of cellulose I and the higher ratio for cellulose I β compared to II and III $_I$ indicates alternate crystalline forms for the latter two samples were achieved. The IR-derived TCI and the XRDss CI values for the three celluloses all are similar in both cases and indicative that the three samples have similar amounts of their respective crystalline forms. While highlighting this observation is straightforward, it remains important because the assessments in the remainder of this data set all assume that differences between the cellulose allomorphs are the primary

Fig. 1 Normalized XDR (a) and ATR-IR (b) spectra for the prepared celluloses I β , II, and III $_I$

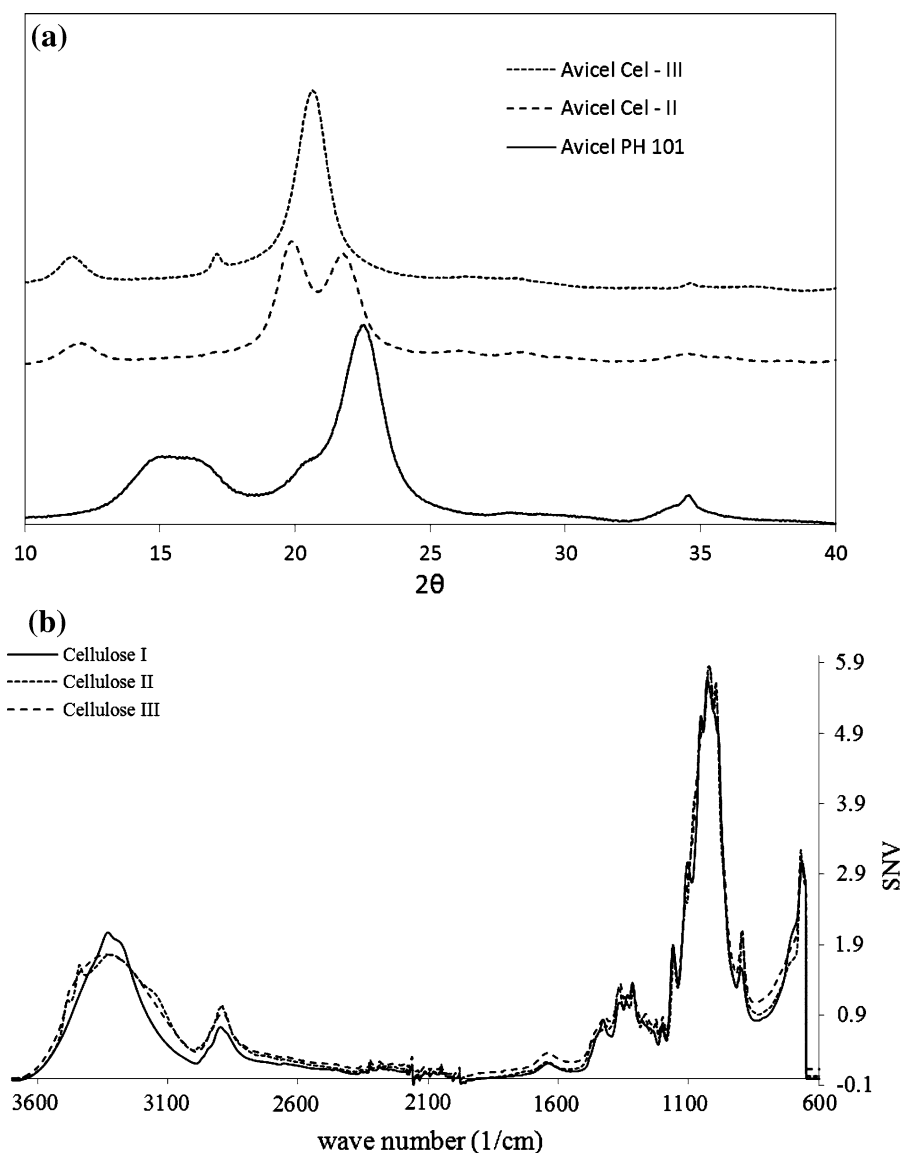


Table 1 Values of the crystallinity indexes (CI) for the cellulose samples used in this study determined from XRD and ATR-IR spectra

Cellulose sample	CI-XRD	LOI-IR	TCI-IR
Cellulose I β	64.8	0.49	1.4
Cellulose II	66.6	0.33	1.22
Cellulose III _I	65.1	0.38	1.39

cause of hydration disparities and not varied levels of crystalline cellulose itself.

Comparative enzymatic saccharification

Comparison of 24 h hydrolysis data for the cellulose allomorphs in Fig. 2 is revealing. At an enzyme loading of 10 mg/g cellulose, saccharification was more efficient for cellulose III_I compared to the other allomorphs. In addition, the impact of increased initial dry solids does not appear to be as significantly detrimental with respect to cellulose III_I as compared to cellulose I β and II. This data is in agreement with other studies that have also shown cellulose III_I to be the most effectively hydrolyzed by synergistic cellulase mixtures (Mittal et al. 2011; Chundawat et al. 2011). Igarashi et al. (2007) hypothesized that reduced crystallinity, lower packing density, and greater distance between hydrophobic surfaces may contribute to improved conversions for cellulose III_I; these latter two factors may help explain our observations at

higher dry solids loadings. While the hydration data to follow can provide some further insight, we would like to remind here that the cellulose allomorphs utilized in this study were prepared with identical crystallinity levels making it apparent that reduced cellulose crystallinity alone is likely not the fundamental basis for the well-documented enhancement in conversion rates for cellulose III_I.

Hydration of the cellulose allomorphs

DVS hydration data on the cellulose allomorphs is presented in Fig. 3. Here it is clear that the cellulose II allomorph has a higher water sorption capacity than the cellulose I β and III_I allomorphs. In addition, data in Fig. 3 also indicate that water uptake is slightly greater at lower humidity levels in cellulose I β and III_I as compared to cellulose II (shown in “Zoomed View” in Fig. 3). This may be indicative of slightly higher amounts of tightly bound surface water per unit mass in these cellulose allomorphs as compared to cellulose II, but differences in the adsorption curves at these humidity levels are so slight that this should be only considered a notable observation and cannot be stated with strong certainty.

In Fig. 4a, b, the LF-NMR relaxometry data for 30 % (w/w) cellulose slurries agree well with the data obtained by DVS. Of the three different cellulose allomorphs the cellulose II sample constrains, or restricts, the system water the most resulting in the

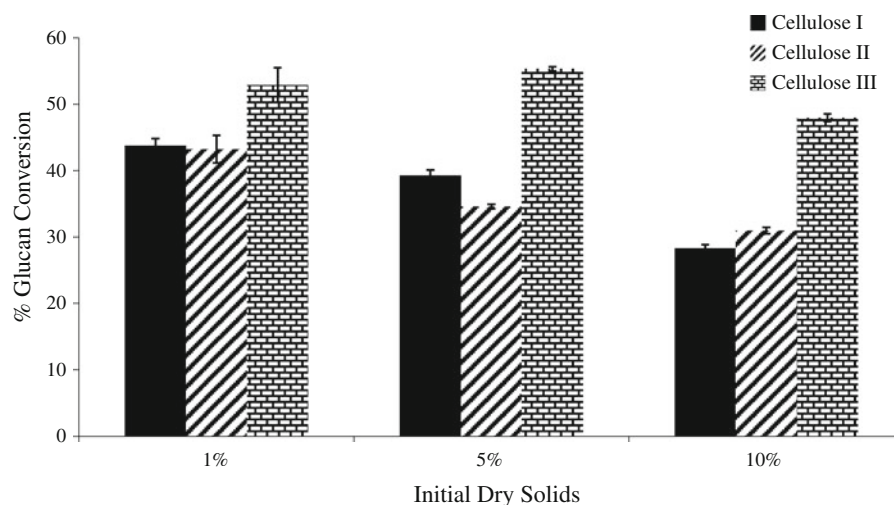
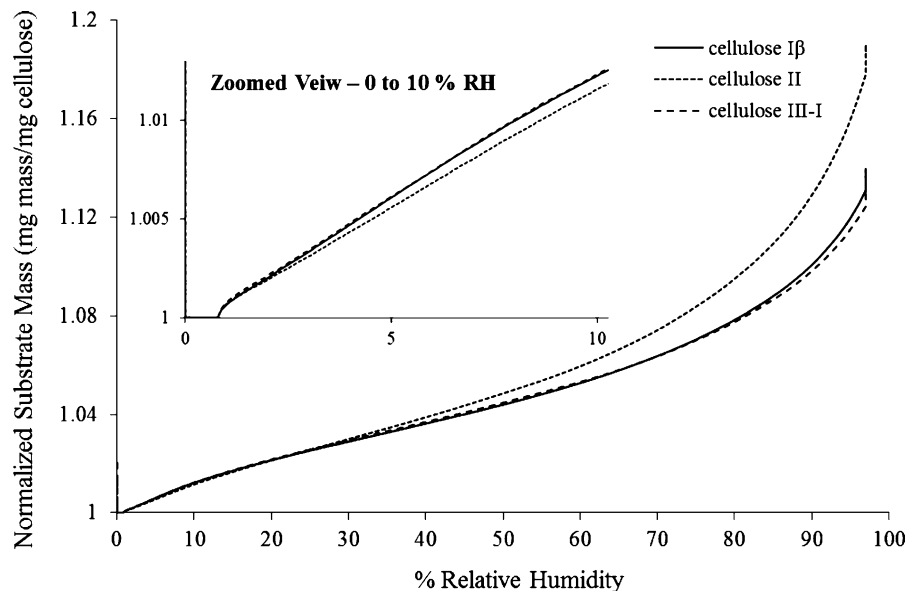


Fig. 2 24 h enzymatic conversion extents achieved at 48 °C, pH 4.8, by a 10 mg/g cellulose loading of commercial cellulase for I β , II, and III_I at varied initial dry solids loadings

Fig. 3 Water vapor sorption isotherms for crystalline cellulose I β , II, and III $_I$



tightest or most quickly relaxing overall CPMG profile with respect to time. Following cellulose II, cellulose I β may be the next most constraining. This order with respect to overall water constraint reflects well with the DVS data showing the holding capacity of the cellulose allomorphs for water to be similar in order.

From the CONTIN spin–spin relaxation time distribution profiles in Fig. 4b we can see that the cellulose III $_I$ allomorph results in the largest peaks at the longer relaxation times (i.e. above 500 ms) for 30 % (w/w) dry solids loadings; according to Felby et al. (2008) these relaxation times are associated with the free water present in a system. This becomes understandable when you consider that cellulose III $_I$ takes up the least water on a per gram basis amongst the three cellulose allomorphs (Fig. 3). The additional “free”, or unbound, water may be beneficial in high solids systems where less water is thought to be freely available for biological reactions to take place (Selig et al. 2012).

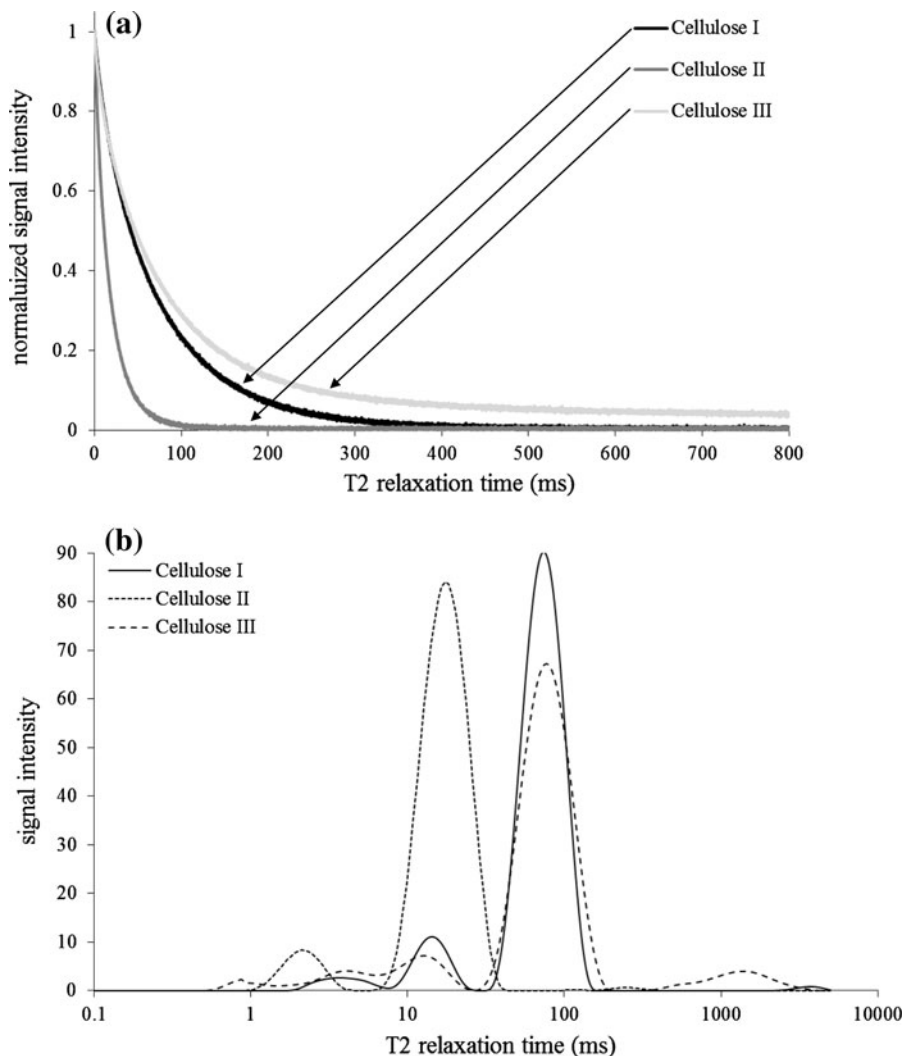
When observing the hydration profiles of the cellulose allomorphs it is apparent that the holding capacity for water differentially affects the constraint of the system water when the moisture contents are held identical. Despite this, it is not necessarily an accurate comparison of how tightly bound the surface water in each system is. In all cases the varied levels of “free water” will have an effect on the overall constraint of all water molecules in a system. In the Fig. 4b profiles we can see that cellulose III $_I$ has the greatest abundance of “free” water present at 30 % (w/w) dry solids. At the

same time, the cellulose III $_I$ allomorph appears to produce the most constrained pool (peak) of water centered around a relaxation time of about 1 ms; this is likely associated with the most tightly bound surface-bound water on the cellulose. The average relaxation time (from triplicate runs) that this most constrained (fastest relaxing) water peak emerges for each cellulose allomorph was ~ 0.7 ms (SD ~ 0.3 ms), 1.1 ms (SD ~ 0.2 ms), and 3.1 ms (SD ~ 1.6 ms) for cellulose cellulose III $_I$, II, and I β respectively.

The above observation was further repeated at 10 % (w/w) solids in the hydrolysis LF-NMR (Fig. 5a–c). At this water content, the fastest relaxing water peak, or most constrained peak, of the initial time-point (hydrolysis after 10 min) profile for cellulose III $_I$ (5C) emerges at an average relaxation time of 10.6 ms (SD ~ 1.2 ms) while similar peaks for the cellulose I β and II allomorphs emerge at average relaxation times of 13.9 ms (SD ~ 1.6 ms) and 16.4 ms (SD ~ 3.1 ms), respectively. While the LF-NMR experimental sets mentioned above consistently indicate that cellulose III $_I$ produces the fastest relaxing pool of water, we should note that the lower part of spin–spin relaxation time distribution is generally less consistent and reliable than portions of the profile at higher relaxations times, and, furthermore, data at relaxation times near or below 0.1 ms are generally erroneous, not repeatable, and were not included in the presented analysis.

The hydrolysis-related T2 distribution profiles in Fig. 5 may also provide some insight into the higher

Fig. 4 (a) CPMG at 30 % initial dry solids, 40 °C. (b) CONTIN T2 distributions for cellulose I β , II, and III_I at 30 % (w/w) dry solids. Profiles presented are from averaged replicate runs on each cellulose

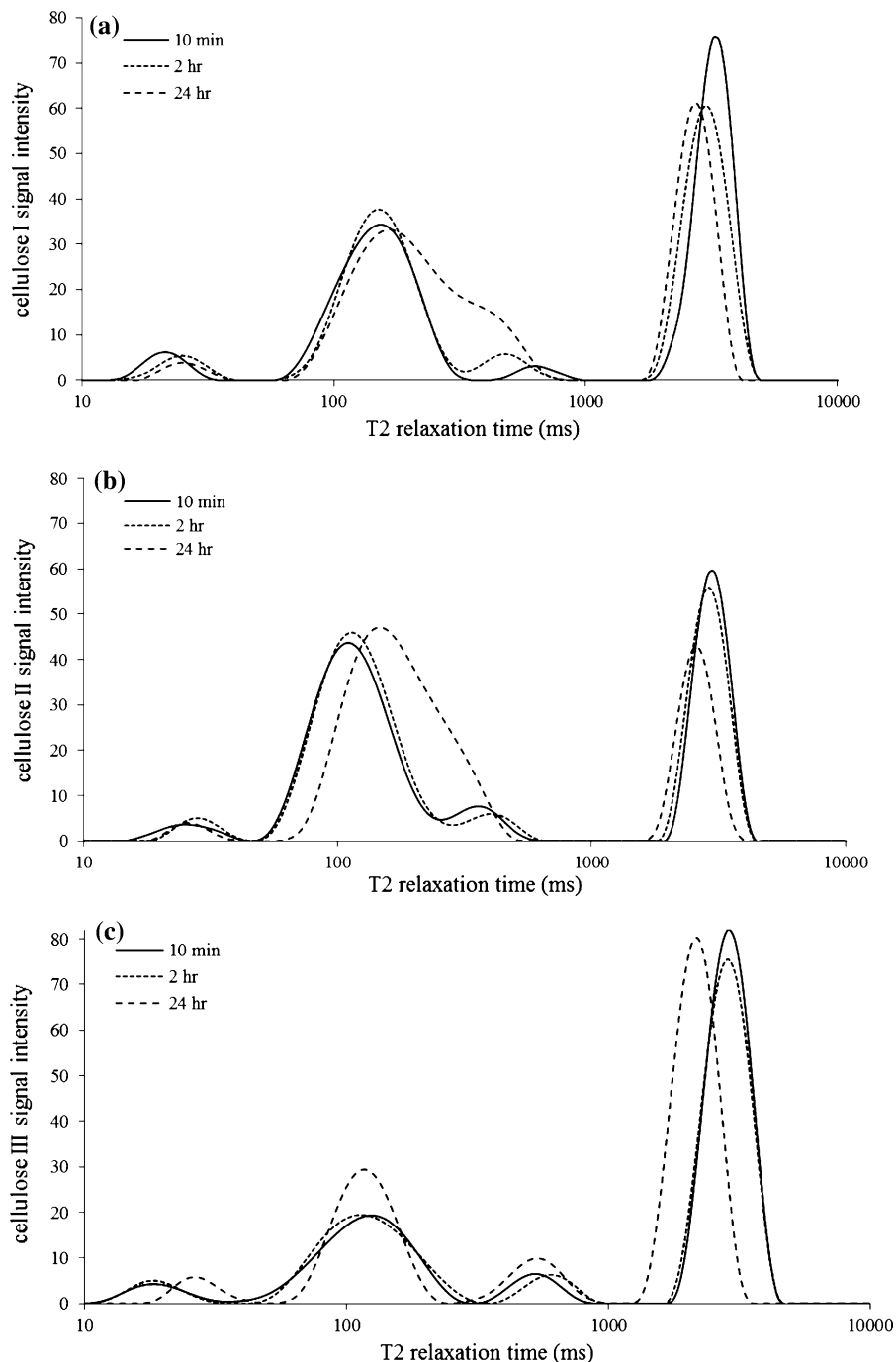


conversions achieved with cellulose III_I versus I β and II. The peaks in the CONTIN profiles for celluloses I β and II appear to shift more similarly to each other than those for the more readily hydrolyzed cellulose III_I. In Fig. 5a, b, the water peaks with relaxation times around 100 ms, thought to be most associated with capillary restricted water, all broaden and shift outwards to longer relaxation times while the same peak for cellulose III_I in Fig. 5c narrows and remains more stationary. We hypothesize that this observation may be indicative of a greater dismantling and broadened variation of the cellulose capillary macro-structure in crystalline forms I β and II compared to III_I. Furthermore, the narrowing of the 100 ms peak in Fig. 5c may indicate a narrowing distribution or increased uniformity in size and form of the cellulose III_I macro-structure. This narrowing of the

capillary water peak around 100 ms at 10 % (w/w) initial dry solids for cellulose III_I is similar to what Felby et al. (2008) observed for cellulose I (filter paper sections) at a much higher dry solids loading of 33 % (w/w) and in the case presented here it appears that at lower solids the greater abundance of water may allow for a more significant diversification of the capillary water pools (near 100 ms) in cellulose I β and II. Overall, these results at 10 % (w/w) initial dry solids are in line with their observation that enzymatic hydrolysis does affect both the surface bound and capillary constrained water pools associated with celluloses.

Changes in the most constrained pools of water represented by the earliest peaks (10–15 ms) (Fig. 5a–c) may also be indicative of greater changes in the microcrystalline structure of cellulose III_I during

Fig. 5 Average LF-NMR data from 24 h saccharifications of the cellulose allomorphs; CONTIN spin–spin T2 relaxation time distributions are plotted for (a) cellulose I β , (b) cellulose II, and (c) cellulose III $_1$



enzymatic hydrolysis. Here, this peak shifts to longer relaxation times in a much more dramatic fashion in the cellulose III $_1$ profile than it does for celluloses I β and II, respectively, the peak crests move from ~21 to 24, 24 to 27, and 17 to 26 ms for cellulose I β , II and III $_1$. While this observation may be simply a product of the greater

hydrolysis extent observed with cellulose III $_1$, and the potential for a subsequent increase in the average pore size, it could also be hypothesized that it is indicative of a greater change in, or even a diminishing of, the most water-constraining surfaces of the cellulose. This may further allow for speculation on the hypothesis that the

most water-constraining surfaces are the most efficiently hydrolyzed. If verifiable, this hypothesis would also add strength to a previous hypothesis we have made placing the blame on the movement of water away from substrate surfaces for observed decreases in conversion efficiencies at high dry matter concentrations (Selig et al. 2012).

With the focus of this paper being solely associated with commercially-prepared cellulose and crystalline allomorphs prepared from it, it is worthwhile summarizing the results in a context that is applicable to industrial lignocellulosic conversion processes themselves. The most notable findings in this regard include a reaffirmation of previous studies showing cellulose III is more readily hydrolysed than other cellulose crystalline forms and more importantly that the enzymatic conversion of cellulose III is less affected by increasing dry solids concentrations than cellulose I or II. This latter point is critical since numerous studies have highlighted the need for industrial lignocellulosic conversion processes to operate at high dry matter loadings as well as the problematic reductions in conversion often observed at such dry solids concentrations (Jørgensen et al. 2007; Hodge et al. 2008). Our data indicate that pretreatment processes, that can effectively convert the I β cellulose present in native lignocelluloses to cellulose III, may be more effective at industrially-relevant dry matter loadings than those where residual cellulose is in another form. Lastly, data from this study, suggest that the comparatively better hydrolysis of cellulose III₁ may be related to differences in hydration behavior compared to I β and II, is in line with previous papers highlighting the criticality of water in industrial-scale bioconversion processes (Felby et al. 2008; Roberts et al. 2011). Overall, the consistencies in this respect with previously published works and the questions raised by this set of data highlights the need for a greater understanding of water dynamics in enzymatic lignocellulose conversion processes.

Acknowledgments We would like to thank Peter Westh and the laboratory at the University of Roskilde for their instruction and permission to use their DVS system.

References

- Atalla RH (1974) Annealing and increased order in cellulose II. *Polym Sci Polym Lett* 12:565–568
- Barnes RJ, Dhanoa MS, Lister SJ (1989) Standard normal variate transformation and de-trending of near-infrared diffuse reflectance spectra. *Appl Spectrosc* 43(5):772–777
- Chundawat SPS, Bellesia G, Uppugundla N, Sousa LC, Gao D, Cheh AM, Agarwal UP, Bianchetti CM, Phillips GM, Langan P, Balan V, Gnanakaran S, Dale BE (2011) Restructuring the crystalline cellulose hydrogen bond network enhances its depolymerization rate. *J Am Chem Soc* 133:11163–11174
- Felby C, Thygesen LG, Kristensen JB, Jørgensen H, Elder T (2008) Cellulose-water interactions during enzymatic hydrolysis as studied by time domain NMR. *Cellulose* 15(5):703–710
- Hodge DB, Karim NM, Schell DJ, McMillan JD (2008) Soluble and insoluble solids contributions to high-solids enzymatic hydrolysis of lignocellulose. *Biores Technol* 99:8940–8948
- Igarashi K, Wada M, Samejima M (2007) Activation of crystalline cellulose to cellulose III₁ results in efficient hydrolysis by cellobiohydrolase. *FEBS J* 274:1785–1792
- Jørgensen H, Vibe-Pedersen J, Larsen J, Felby C (2007) Liquefaction of lignocellulose at high-solids concentrations. *Biotechnol Bioeng* 96:862–870
- Matthews JF, Skopec CE, Mason PE, Zuccato P, Torget RW, Sugiyama J, Himmel ME, Brady JW (2006) Computer simulation studies of microcrystalline cellulose Ib. *Carbohydrate Res* 341:138–152
- Mittal A, Katahira R, Himmel ME, Johnson DK (2011) Effects of alkaline or liquid-ammonia treatment on crystalline cellulose: Changes in morphology, crystallinity index, and enzymatic digestibility. *Biotechnol Biofuels* 4(41):1–16
- Park S, Johnson DK, Ishizawa CI, Parillan PA, Davis MF (2009) Measuring the crystallinity index of cellulose by solid state ¹³C nuclear magnetic resonance. *Cellulose* 16:641–647
- Park S, Baker JO, Himmel ME, Johnson DK (2010) Cellulose crystallinity index: measurement techniques and their impact on interpreting cellulase performance. *Biotechnol Biofuels* 3(10):1–11
- Provencher SW (1982) Contin: a general purpose constrained regularization program for inverting noisy linear algebraic and integral equations. *Comput Phys Commun* 27:229–242
- Roberts KM, Lavenson DM, Tozzi EJ, McCarthy MJ, Jeoh T (2011) The effects of water interactions in cellulose suspensions on mass transfer and saccharification efficiency at high solids loadings. *Cellulose* 18:759–773
- Selig MJ, Hsieh CC, Thygesen L, Himmel ME, Felby C, Decker SR (2012) Considering water availability and the effect of solute concentration on high solids saccharification of lignocellulosic biomass. *Biotechnol Prog* 28(6):1478–1490